A MULTIBAND-INSTABILITY-MONITOR FOR HIGH-FREQUENCY INTRA-BUNCH BEAM DIAGNOSTICS

Ralph J. Steinhagen, CERN, Geneva, Switzerland,
Mark J. Boland, Australian Synchrotron, Clayton, Victoria, Australia
Thomas G. Lucas, The University of Melbourne, Melbourne, Australia

Abstract

The maximum beam particle intensity and minimum emittance that can be injected, accelerated and stored in high-brightness lepton as well as high-energy hadron accelerators is fundamentally limited by self-amplifying beam instabilities, intrinsic to unavoidable imperfections in accelerators. Traditionally, intra-bunch or head-tail particle motion has been measured using fast digitizers, with even using state-of-the-art technology being limited in their effective intra-bunch position resolution to few tens of um in the multi-GHz regime.

To improve on the present signal processing, a multiband-instability-monitor (MIM) prototype system has been designed, constructed and tested at the CERN Super-Proton-Synchrotron (SPS) and Large Hadron Collider (LHC). The system splits the signal into multiple equally-spaced narrow frequency bands that are processed and analysed in parallel. Working with narrow-band signals permits the use of much higher resolution analogue-to-digital-converters that can be used to resolve nm-scale particle motion already during the onset of instabilities.

INTRODUCTION

For very high beam intensities, in addition to single-particle the beam can also suffer from more significant collective effects [1]. A notable collective interaction is the *Head-Tail* instability phenomenon which is caused by a resonance condition in circular accelerators, created by the interplay between beam induced transverse wake fields and longitudinal synchrotron oscillation of the particles within a bunch. The effect, first theorised at the ACO and Adone lepton storage rings [2, 3], was later directly observed at the CERN Proton Synchrotron (PS) and Booster (PSB) (both hadron accelerators)[4, 5, 6]. While the MIM principle covers any generic intra-bunch effects common in circular accelerators, we focus for the discussion of the diagnostics principle on the special case of head-tail (HT) instabilities for vanishing chromaticity and azimuthal modes.

TIME-DOMAIN DETECTION

Historically, the first direct observation of intra-bunch motion were done in time-domain, using wide-band transverse beam position pick-ups connected to an RF hybrid (effectively generating an analog difference Δ and sum Σ signal between two opposing electrodes) and acquired by fast oscilloscopes [4, 7].

The bunches in the PSB, PS, and most low-energy hadron accelerators are typically very long, with base-lengths B typically in the order of 200 ns (assuming a longitudinal $\rho(t) \sim cos^2(\pi t/B)$ distribution). For these long bunches, system bandwidths around 150 MHz were typically sufficient to resolve these intra-bunch instabilities. However, the required bandwidth scales inversely with the bunch length, and the exploitation of the same basic detection principle in high energy proton (LHC: $B \lesssim 1\,\mathrm{ns}$) accelerators and lepton accelerators (i.e. Australian Synchrotron (SLSA) $B \lesssim 120\,\mathrm{ps}$) implies the use of digitizers operating at analog bandwidths of 6-12 GHz (LHC) or above 30 GHz (SLSA). Figure 1 shows simulated time- and corresponding frequency-domain difference signals for a *rigid bunch*, as well as intra-bunch oscillation modes.

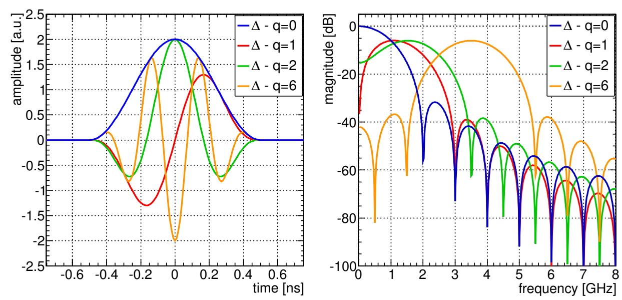

Figure 1: Simulated LHC intra-bunch time-domain and corresponding frequency-domain position signals. The given radial mode number $q = 0, 1, 2$ and 6 correspond to the number of stable fix-points (or zero-crossings) [4, 5, 6].

At these speeds, the effective resolution of even state-of-the-art technology limits the effective intra-bunch position resolution to a few tens of micro-metres. In addition, the expected technology margin for further improvement is diminishing, since the maximum achievable effective number of bits (ENOB) for a given bandwidth is approaching fundamental physical thermal noise and jitter limitations indicated in[8, 9]. For the LHC beam, particle oscillations at this scale cause partial or total loss of the beam due to the tight constraints imposed on transverse oscillations by the LHC collimation system protecting the LHC's sensitive cryogenic aperture.

Where synchrotron-light is available, the state-of-the-art of intra-bunch diagnostics is presently defined by streak cameras [10]. Being versatile and excellent research tools, that can provided equivalent bandwidths in the order of a few 100 GHz, their use is limited to ad-hoc measurements rather than continuous monitoring of instabilities occurring at an a-priori unknown time. Also, these are limited in their dynamic range, robustness with respect to largely varying signal levels, non-real-time post-processing, and total recording length of a few bunches and turns.

ISBN 978-3-95450-127-4

Copyright © 2013 by JACoW — cc Creative Commons Attribution 3.0 (CC-BY-3.0)

MIM PRINCIPLE

As can be seen in Fig. 1, the maxima of the HT motion in the frequency domain shift towards higher frequencies for increasing detail of intra-bunch motion. This dependence can be used to distinguish between a rigid-bunch and intra-bunch oscillation mode by comparing the amplitude ratios of the longitudinal carrier with the given transverse side-band modulation of only two frequency bands, as shown in Fig. 2. For the rigid-bunch mode the ratio between the carrier and side-band is constant for all frequencies, whereas for the intra-bunch oscillations, the ratio typically varies with frequency. More specifically, by correlating the frequency maxima of the Δ signal with the given carrier signal distribution of the Σ channel, the given head-tail instability mode number can be derived.

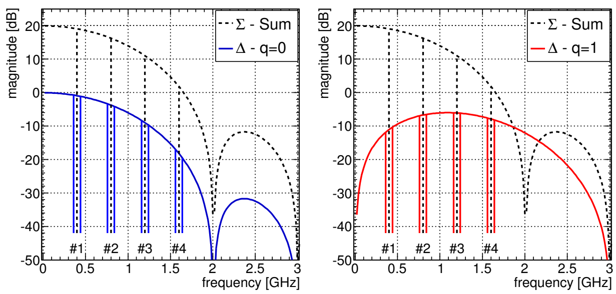

Figure 2: Simulated difference- (Δ) and sum- (Σ) frequency domain signals for a rigid bunch ($q = 0$) and intra-bunch ($q = 1$) head-tail mode motion. The carrier frequency (black, dashed) and side-bands (red,blue) are indicated. Distance between carrier and side-band not to scale.

The developed MIM exploits this property in frequency-domain and splits the analog input signal from a beam position sensitive pick-up into multiple equally-spaced narrow frequency bands, that are processed and analysed in parallel, as schematically illustrated in Fig. 3. Each band is amplified to compensate for filter coupling losses and reduced signal levels at higher frequencies due to the given bunch distribution. Working with narrow-band signals in frequency-domain permits the use of higher-gain low-noise amplifiers, more flexible RF filters, impedance transformation, and much higher resolution analogue-to-digital-converters.

Similar analog front-end solutions have been independently studied in the context of RF radio receivers, sometimes referred to as *cochlear radio* in reference to being inspired by nature's design of the inner ear (*lat: cochlea*) of mammals [11, 12, 13, 14].

In contrast to narrow-band quasi-continuous-wave RF radio signals, beam signals are essentially pulsed wide-band RF signals, and the MIM can thus deploy certain additional specific optimisation that limit the total number of required bands and their overlap, notably:

(a) the shortest physically possible bunch length B_{min} defines the maximum required Nyquist-Shannon bandwidth f_{NQ} that contains e.g. 99 % of the signal power,

(b) the maximum bunch length is finite and given by the size of the stable RF phase-space separatrix B_{max}, which defines the minimum instantaneous frequency resolution $\Delta f_b|_{min} = 1/B_{max}$ that can be resolved within a single passage of the bunch, and

(c) the minimum separation between bunches defines the minimum required bandwidth Δf_{BW} or filter quality factor to separate between two consecutive bunches.

Based on the nominal LHC (SPS) design parameter of $B_{min} \gtrsim 0.8(1.6)\,\text{ns}$ (or $\sigma_t \gtrsim 0.2(0.4)\,\text{ns}\ r.m.s.$), $B_{max} = 1/f_{RF} = 1/400(200)\,\text{MHz} = 2.5(5)\,\text{ns}$, and typical 40 MHz bunch repetition frequency, the time-domain signal can be unambiguously be reconstructed from a down-sampled version of frequency domain data for a MIM consisting out of 32 bands, spaced by $\Delta f_b = 400\,\text{MHz}$, individual bandwidth of each band of $\Delta f_{BW} \gtrsim 100 - 200\,\text{MHz}$ and overall theoretically bandwidth of just above 12 GHz. For the nominal system to be deployed, each output will be split into two: one narrow-band channel optimised for sensitivity, and the other for wide-band bunch-by-bunch acquisitions. The main purpose of the first channel is to provide an indication of the onset of instabilities, their amplitude and growth time in order to correlate these with other instruments, while the second will provide more generic and detailed information for each given bunch.

While very wide-band pick-ups are under study that aim at providing an effective bandwidth in excess of 12 GHz [15], the presently available strip-line pick-ups, hybrids and cabling infrastructure supports only $f_{max} \approx 6\,\text{GHz}$, limiting the number of "useful" channels with adequate signal levels to 16. Still, the expected reconstruction error for typical time-domain signals using only a sub-set of 16 discrete frequency bands is below the few percent level, as illustrated in Fig.. 4.

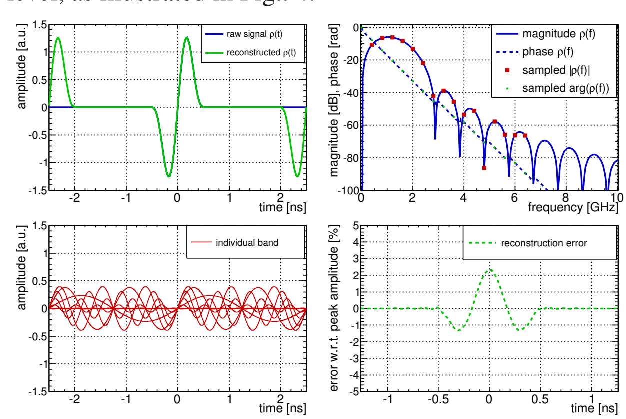

Figure 4: Generic MIM example: the original and reconstructed signal (top left), their frequency domain representation and sub-sampling (top right), contribution of the individual bands (bottom-left), and reconstruction error (bottom right) excluding mirror images are shown.

During the end of the final-focus squeeze of most LHC fills, a set of few isolated bunches was affected by instabilities, losses and/or emittance growth. The MIM prototype

Copyright © 2013 by JACoW — cc Creative Commons Attribution 3.0 (CC-BY-3.0)

ISBN 978-3-95450-127-4

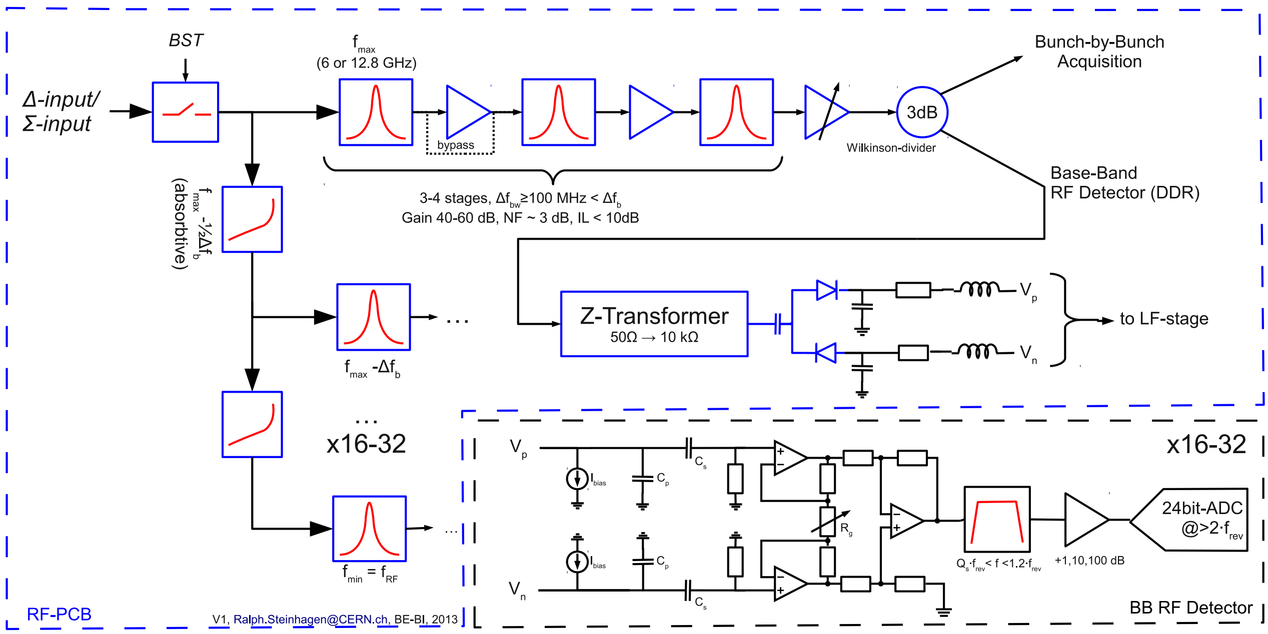

Figure 3: Multiband-Instability-Monitor (MIM) Schematic.

was initially intended as proof-of-concept to better diagnose these instabilities, and to assess whether these instabilities are caused by rigid- or intra-bunch motion using a limited number of bands. Thus only the narrow-band acquisition chain was deployed, and with a limited number of bands located at 0.4, 0.8, 1.2 and 1.6 GHz, plus two broad-band channels. While the system is capable of resolving signals on a bunch-by-bunch basis, the amplified signals of each band have been down-mixed for simplicity and robustness using a custom, narrow-band RF Schottky Diode Peak Detector [16, 17, 18], prior to being amplified and band-pass filtered by a instrumentation amplifier, and digitised by an 24-bit ADC. In order to recover the carrier signal, needed to normalise and compare the oscillation between the individual bands, the signal has been sampled above three times the revolution frequency. A fast RF-switch prior to the filter bank allowed gating to study specific bunches.

SPS AND LHC BEAM EXPERIMENTS

The first functional tests were performed at the SPS, inspired by and in comparison to earlier tests with base-band-tune meter (BBQ, [19]). These indicated a much higher sensitivity for beam oscillations and often small amplitude tune signals that – beside for some cases with the Schottky monitor – could not be measured by other traditional time-domain BPM-acquisition systems. Figure 5 shows such a tune signal taken with the MIM for a full-bandwidth and a band at 400 MHz. The vertical tune $Q_v = 0.585$ and horizontal tune $Q_h = 0.625$ fixed-target tunes, and their lower f_{rev} side-band copies are visible. Both spectra have been normalised to the revolution carrier. Then higher side-band to carrier ratio at high frequency suggests the detection of intra-bunch motion as depicted in Fig. 2.

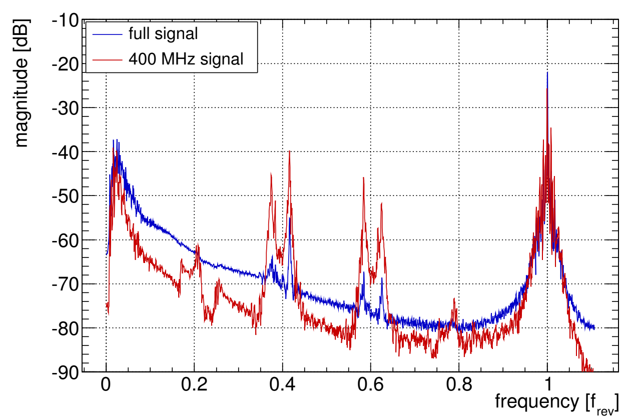

Figure 5: SPS MIM measurement example (2013-09-09).

The system was subsequently installed in the LHC and used to monitor the above mentioned instabilities for beam 1 in the vertical plane. Figure 6 shows the corresponding MIM spectra at 0.4 and 1.2 GHz for one instability occurring at the end of the LHC final-focus squeeze. The tune and side-band oscillation structure are significantly more pronounced for the 1.2 GHz.

Besides detecting intra-bunch instabilities, the system has been also tested to measure the stability margin for driven intra-bunch modes. For this purpose, a wide-band RF power amplifier has been installed, driving a 1 m long strip-line kicker structure in order to perform beam-transfer-function measurements (BTF) and to detect the growth or damping time of the specific intra-bunch motion. Figure 7 shows the measured spectra evolution for one MIM channel during one of the experiments. The exciter frequency was slowly chirped across the tune resonance at 0.4, 0.8 and 1.2 GHz, corresponding to some of the expected head-tail modes indicated in Fig. 1. For the exper-

ISBN 978-3-95450-127-4

Copyright © 2013 by JACoW — cc Creative Commons Attribution 3.0 (CC-BY-3.0)

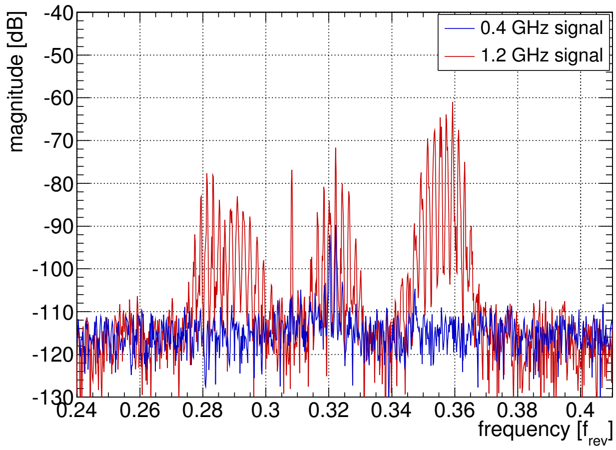

Figure 6: LHC MIM measurement example (2012-12-04, end of final-focus squeeze, Fill 3374).

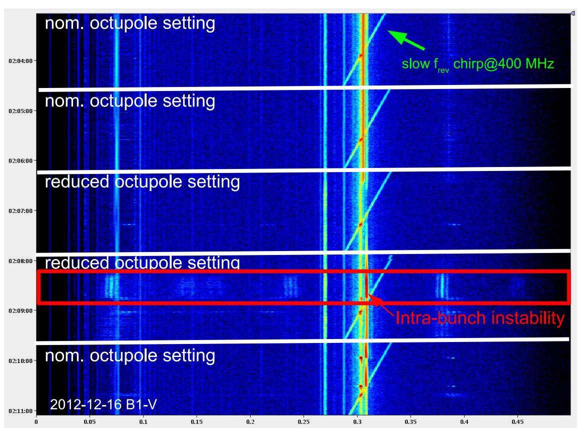

Figure 7: MIM measurement example for a driven intra-bunch instability (2012-12-16, B1, vert.). The plot shows the beam oscillation (amplitudes are colour coded) as a function of frequencies normalised to f_{rev} and time. Diagonal lines correspond to slow BTF scans.

iment, the octupole settings were initially kept at their original value suppressing the instabilities, and then reduced for the subsequent BTF scans. The resonant enhancement of the tune line whenever the slow BTF excitation passes $Q_v = 0.305$ is visible. An oscillation with growth times of a few minutes is visible during the third BTF scan while crossing $0.31 f_{rev}$ and that builds up to a full blown instability by the time of the fourth BTF scan. The additional harmonics during the instability are probably due to saturation effects in the RF diode detector and instrumentation amplifier. Subsequent scans trigger more instabilities that self-stabilise similar to what was observed during regular operation at the end of the final-focus squeeze.

CONCLUSION

Initial measurements with the MIM seem to indicate that the tune oscillations in the SPS and instabilities at the LHC are related to intra-bunch beam motion. First measurements of the driven intra-bunch motion are promising and could potentially be exploited to evaluate machine settings and their impact on beam stability.

The initial operational system to be deployed will rely on a (gated) direct-down-conversion, and targets to provide an indication of the onset of instabilities, their amplitude and growth time in order to correlate these with other beam instruments. Further simulation studies are required to evaluate whether magnitude-only information is sufficient to adequately identify bunch-by-bunch intra-bunch instability or whether full amplitude-and-phase detection is necessary.

ACKNOWLEDGEMENTS

The authors express their thank and gratitude to Bengt E. Jonsson (ADMS Design), Marek Gasior, Philippe Lavanchy, Elias Metral, and Philippe Semanaz (CERN) for the fruitful discussions, advice and help during the construction of the first prototype.

REFERENCES

[1] Elias Metral in: "Elementary Particles - Accelerators and Colliders", Chapter 4, Landolt-Bornstein, Vol. 21, Springer, London, ISBN-9783642230523, 2013

[2] M. Sands, SLAC-TN-69-008 & SLAC-TN-69-010, 1969

[3] C. Pellegrini, Nuovo Cim. A64 (1969) 447-473

[4] J. Gareyte, CERN-MPS-BR-74-7, CERN, 1974

[5] F. J. Sacherer, CERN-MPS-INT-BR-74-8, CERN, 1974,

[6] F. J. Sacherer, CERN/PS/BR 76-21, CERN, 1976,

[7] J. Borer, ISR-RF-TH-JB-AH-ps, CERN, 1975

[8] Bengt E. Jonsson, "ADC performance evolution: Sampling rate and resolution", Converter Passion, 2012-08-16, available at: http://converterpassion.wordpress.com/

[9] Anatol Khilo et al., "Photonic ADC: overcoming the bottleneck of electronic jitter", Optics Express, Vol. 20, No. 4, February, 2012

[10] Bingxin Yang, BIW'06, AIP Conference Proceedings, Volume 868, pp. 124-137, 2006

[11] Scott R. Veluzquez, "High-performance advanced Filter Bank Analog-to-Digital Converter for Universal RF Receivers", IEEE-SP TFTS, Pittsburgh, PA, USA, 1998

[12] S. Mandal et al., "A Bio-Inspired Active Radio-Frequency Silicon Cochlea", IEEE SSC, VOL. 44, NO. 6, 2009

[13] D. F. Albuquerque et al., "Cochlear Radio", EuMW – European Wireless Technology Conference, Paris, France, 2010

[14] D. F. Albuquerque et al., "Analog Filter Bank for Cochlear Radio", RF Front-ends for Software Defined and Cognitive Radio Solutions (IMWS), IEEE, 2010

[15] Steinhagen et al., "Application of Metal-Semiconductor-Metal (MSM) Photodetectors [..]",these proceedings

[16] Wes Hayward and Dick Bingham, "Direct Conversion - A Neglected Technique", ARRL, QST, Nov, 1968

[17] M. R. Barber et al., IEEE G-MTT, Vol. 66, No. 1, 1966

[18] Mark R. Barber, IEEE MTT, Vol. 15, No. 11, 1967

[19] M. Gasior and R. Jones, CERN-LHC-Project-Report-853, CERN, 2005

Copyright © 2013 by JACoW — cc Creative Commons Attribution 3.0 (CC-BY-3.0)

ISBN 978-3-95450-127-4